J of Nuclear Medicine Technology, first published online December 21, 2021 as doi:10.2967/jnmt.120.261893

Title: Global and Regional Variations in Transthyretin Cardiac Amyloidosis: A Comparison of Longitudinal Strain and ^{99m}Technetium Pyrophosphate Imaging.

Short Running Title: *A comparison of ECHO strain imaging and ^{99m}Technetium Pyrophosphate*

Authors: [*] Christopher Lee[1] MD, [*]Chieh-Ju Chao[1] MD, Pradyumna Agasthi[1] MD, Amith R Seri[1], MD, Amar Shere[1] MD, Lanyu Mi[2] MS, Lisa Brown[1] RDCS, Chance Marostica[1], Timothy Barry[1] MD, Ming Yang[3] MD, Julie Rosenthal[1] MD, Samuel Unzek[4] MD, Farouk Mookadam[1] MB BCh, and Reza Arsanjani[1] MD

[1] Department of Cardiovascular Diseases, Mayo Clinic Arizona

[2] Department of Research, Division of Biomedical Statistics and Informatics, Mayo Clinic Arizona

[3] Department of Radiology, Mayo clinic Arizona

[4] Banner – University medical Center Phoenix

[*]The two authors have the same amount of contribution to this manuscript.

Conflict of interest disclosure

The authors declare they do not have anything to disclose regarding conflict of interest with respect to this manuscript.

Address for Correspondence:

Reza Arsanjani MD

Mayo Clinic Arizona

Department of Cardiovascular Disease

5881 E Mayo Blvd, Phoenix, AZ 85054

Abbreviations

CA: cardiac amyloidosis

h-TTR: hereditary transthyretin

wt-TTR: wild-type transthyretin

CM: cardiomyopathy

GLS: global longitudinal strain

RLS: regional longitudinal strain

RALSI: relative apical longitudinal strain index

^{99m}Tc-PYP: ^{99m}Technetium Pyrophosphate

TTE: transthoracic echocardiogram

HMDP: Hydroxymethylene diphosphonate

Abstract

Background: There is limited data on the head-to-head comparison of ^{99m}Tc-pyrophosphate (PYP) and echocardiographic strain imaging in the assessment of transthyretin (TTR) cardiac amyloidosis.

Methods: At Mayo Clinic Arizona, patients that had undergone both a ^{99m}Tc-PYP scan and transthoracic echocardiogram (TTE) within a 90-day period were retrospectively identified for chart review and strain imaging analysis. Patients were divided into two groups according to their ^{99m}Tc-PYP results (PYP+ and PYP -) for the comparison. A standard 17-segment model was used for segmental, regional, and global longitudinal strain comparison. A p-value of <0.05 was deemed as significant.

Results: A total of 64 patients were included, the mean age was 75.1 ± 13.0 years and 57(89.1%) were male. Comparing the PYP+ to the PYP- group, the left ventricular global longitudinal strain was significantly worse (PYP+ vs. PYP-: -10.5 ± 2.6 vs. -13.1 ± 4.1, p= 0.003). PYP+ patients also had worse regional basal strain (-4.6 ± 2.6 vs. -8.8±4.0, p<0.001) and a trend of worse mid-ventricular strain (-9.6 ± 4.0 vs. -11.7± 4.4, p= 0.07), however, no statistical difference in apical region (-17.6 ± 4.73 vs. -19.0 ± 6.46, p = 0.35). This is consistent with an apical sparing pattern shown by the relative apical longitudinal strain index (1.3 ±0.5 vs. 1.0 ± 0.3, p=0.008). Segment to segment analysis demonstrated significant difference in strain between PYP+ and PYP- segments in 4 segments: basal inferior (p=0.006), basal anterolateral (p= 0.01), apical septal (p=0.002) and apical inferior (p=0.001). Left ventricular diastolic dysfunction was significantly different with 17 (77.3%) patients in group PYP+ versus 15 (36.6%) in PYP- participants (p = 0.002).

Conclusion:

Our study suggested that PYP uptake is related to overall worse LV segmental, regional, and global longitudinal strain function, as well as diastolic function compared to patients without PYP uptake. This provides important data for clinicians to know the echocardiographic function features related to ^{99m}Tc-PYP uptake and can serve as a hypothesis-generating study for future investigators.

Background/ Introduction

Amyloidosis is a heterogeneous group of disorders involving the extracellular deposition of insoluble amyloid protein that can occur in different organs. Amyloidosis can be either inherited or acquired. The cardiac manifestation of amyloidosis includes heart failure, conduction disease, syncope and sudden cardiac death (*1*). So far, while over 30 different amyloidogenic proteins have been described, cardiac amyloid deposition and the development of cardiomyopathy are associated with types of amyloid proteins, most commonly transthyretin (TTR) and amyloid light chain (AL) proteins (*2*).

Concerning the diagnosis of cardiac amyloidosis (CA), endomyocardial biopsy demonstrated amyloid deposition remains the gold standard and is also important for protein typing (*3*). However, newer non-invasive approaches can potentially allow earlier detection of cardiac amyloidosis with minimal side-effect profile. In patients with a non-cardiac biopsy demonstrating amyloid deposition, cardiac involvement has been defined—by a consensus opinion from the 10th International Symposium on Amyloidosis—as either a positive heart biopsy and or increased left ventricular wall thickness (interventricular septal thickness >12 mm) in the absence of hypertension or other potential causes of true left ventricular hypertrophy (*4*). Making an early diagnosis of cardiac amyloid has significant clinical implications, concerning the poor prognosis of late stage CA (*1,5*). However, as of 2019, TTR remained to be underdiagnosed- there were still 10 to 15% of older adults with heart failure may have unrecognized wild type TTR (*5*).

Historically, the diagnosis of CA had involved a high index of clinical suspicion and consideration of a constellation of symptoms. Increased wall thickness noted on the echocardiogram was initially seen as a clue to cardiac amyloidosis, however, the same finding can also happen in different clinical conditions such as hypertrophic cardiomyopathy and hypertensive heart disease (*6,7*) . In clinical practice, a comprehensive evaluation of echocardiography parameters or involving other non-invasive studies are generally required to better differentiate these conditions. The characteristic “apical-sparing” pattern of myocardial strain distribution is suggestive for CA from other etiologies when the initial echo findings raised the concerns (*7-9*). The apical sparing strain pattern, although is often considered as the feature of CA, has been observed in both AL- and TTR-type CA (*10,11*). The difference of myocardial strain dysfunction between different subtypes was also reported (*10*).

The other widely used noninvasive modality is Technetium-Pyrophosphate (^{99m}Tc-PYP) imaging, which is highly sensitive and specific for the diagnosis of TTR-related amyloidosis without the need for endomyocardial biopsy (*12*). A recent Europe study using Tc^{99m}-Hydroxymethylene diphosphonate (^{99m}Tc-HMDP) identified regional distribution of nuclear tracer uptake in patients with TTR-related CM, which was similar to the apical sparing pattern of strain echo imaging (*13*). The difference of the uptake of hTTR and AL cardiac tissues is believed to be related to the microcalcifications in hTTR cardiac tissues, which is more common than AL cardiac tissue (*14*).

Despite being commonly used for the assessment of CA, strain echocardiography and ^{99m}Tc-PYP imaging findings have yet to be compared directly to each other. Differences of echocardiographic parameters were also reported between the AL and TTR subtypes of CA.

We designed the study to compare the echocardiographic strain distribution patterns between patients with positive PYP study (PYP+ group) and negative PYP study (PYP- group) results. We hypothesized that ^{99m}Tc-PYP uptake is correlated to worse echocardiographic left ventricular (LV) strain function.

Methods

This study protocol complies with the Declaration of Helsinki and is approved by the Mayo Clinic institutional review board (IRB). Informed consent was waived as this study was deemed to be minimal risk (retrospective chart review and data analysis only).

Patient Population

A retrospective study of all consecutive patients who had undergone both ^{99m}Tc-PYP scan for suspected cardiac amyloidosis and transthoracic echocardiogram (TTE) within 90 days of each study were selected from a single center (Mayo Clinic, Arizona) in the period of October 2015 to March 2018. Individuals included in the study had high clinical suspicion for cardiac amyloidosis including increased left ventricular wall thickness in the absence of significant hypertension and had findings most suggestive of cardiac amyloidosis rather than hypertrophic cardiomyopathy. These individuals subsequently underwent SPEP, UPEP, and free light chain and were then referred for technetium pyrophosphate scan (*15*).

Each patient's TTE study was reviewed for image quality selection criteria, which included echocardiogram images of acceptable quality of the standard apical 4-, 3-, and 2-chamber views, to allow for complete strain imaging analysis. Adequate quality was defined as no more than 2 segments of unreadable strain, which was the only metric which resulted in otherwise eligible participants being excluded from final analysis.

Patient Demographics, electrocardiograms, biomarkers, and ancillary data

Detailed EHR review yielded a broad dataset including participant demographics (age, gender), body mass index (BMI kg/m^2), creatinine, estimated glomerular filtration rates (eGFR), troponin, N-terminal (BT)-prohormone beta-natriuretic protein (NT-pro-BNP), and clinical parameters including the presence or absence of low-voltage ECG, pleural effusion, and pericardial effusion.

Echocardiography and Strain imaging

Measurement of LV diastolic function including descriptions and acquisition of specific parameters are outlined by *Naguech et al* (16). The original TTE reports were reviewed to obtain echocardiographic structural, systolic and diastolic functional parameters including left ventricular ejection fraction (LVEF, %), LV mass (g), LV mass index (g/m2), LV stroke volume (mL), cardiac index (L/m^2/min), mitral E-wave velocity (m/s), mitral A-wave velocity (m/s), mitral E/A ratio, mitral E wave deceleration time (ms), tissue doppler medial e' velocity (m/s), E/e' ratio medial, E/e' ratio lateral, tricuspid annulus systolic excursion by M-mode (mm), right ventricular systolic pressure (RVSP, mmHg) and the presence of diastolic dysfunction. All of the echocardiographic parameters were measured according to the American Society of Echocardiography guidelines (*17,18*).

Strain imaging was retrospectively completed using a commercial software, Epsilon EchoInsight©. Strain imagining was initially generated utilizing the 18-segment model. Global longitudinal strain (GLS) and regional longitudinal strain (RLS) values for apical, mid and basal were abstracted as reported by EchoInsight©. Both strain and PYP imaging were represented using the standard 17-segment AHA model (*18*). Strain modeling was converted from the 18-segment model to the 17-segment model to allow direct comparability (**Figure 1**). This conversion process involved the average of the strain segments 13 through 18 from the 18-segment model; this average was then taken to represent segments 13 through 17 in the 17-segment model.

^{99m}*Technetium -Pyrophosphate Imaging*

^{99m}Tc-PYP scan was performed using a standard American Society of Nuclear Cardiology (ASNC) protocol containing both planar and Single-photon emission computed tomography/computed tomography (SPECT/CT) series[18]. *After intravenous administration of 370 MBq Tc-99m Pyrophosphate (PYP), 15-minute and 3-hour delayed anterior view planar images of the chest (matrix 256 x 256) were acquired, followed by SPECT/CT scan of the chest.*

On the 3-hour anterior planar image, circular region of intertest (ROIs) were placed around the heart and contralateral right chest to measure the counts and calculate the heart to contra-lateral (H/CL) ratio. H/CL values > 1.4 is considered indicative of TTR CA with a high PPV. H/CL values in the range 1.3-1.4 can be seen with TTR amyloidosis, especially when activity is seen in the myocardium on SPECT/CT.

On SPECT/CT image, the semiquantitative grading (0-3 scale) is based on the visual inspection of tracer uptake level in myocardium compared to that of the rib (19).

Other variables include heart to contralateral lung ratio (H/CL ratio) of the counts at anterior view planar scintigraphy image and SPECT/CT based semi-quantitative scale of the myocardial radiotracer uptake. A positive ^{99m}Tc-PYP scan is defined as any of the 17 segments deemed to be PYP positive according to the ASNC guidelines (*20*). ^{99m}Tc-PYP scan was reported utilizing the bulleyes 17-segment model.

Electrocardiograms, biomarkers, and ancillary data

The electronic health records were reviewed for patient demographic and other clinical data, including participant demographics (age, sex), body mass index (BMI kg/m^2), serum creatinine, eGFR, troponin, NTpro-BNP; clinical parameters including the presence or absence of low voltage ECG, pleural effusion and pericardial effusion.

Statistical Analysis

Descriptive statistics summarized demographic and clinical characteristics. Mean (SD) with two-sample t-test for group comparison was presented for normally distributed continuous variables, and median (interquartile range, IQR) with Wilcoxon rank sum test was used to describe non-normally distributed continuous data. Categorical variables were summarized as frequency (%)

with Fisher's exact test for comparison. As for strain imaging parameters, a two-sample t-test was used for global, regional and segmental analysis. The 17-segments were categorized into three different regions (basal, mid and apical) for regional analysis. Relative apical longitudinal strain index (RALSI) was calculated as average apical LS/average basal LS + average Mid LS[8]. Of note, regional analysis was done to compare mean longitudinal strain in participants with PYP+ in any segment to those with a completely negative ^{99m}Tc-PYP scan. Segment analysis was done to compare mean strain in ^{99m}Tc-PYP positive (PYP+) versus negative (PYP-) participants in each corresponding segment. The analysis was conducted by SAS 9.4 (SAS Institute). All tests were two-sided and a p-value < 0.05 was considered statistically significant.

Pearson correlation between PYP scan findings and strain parameters with graphical illustration is included in the supplemental materials (Table S1 – S4). For PYP- participants, global longitudinal strain is significantly strongly correlated with apical, mid, and basal regions with Pearson correlation coefficient >0.6 and p value <.001. The apical region is significantly strongly associated with mid region, with correlation of 0.7 (p<.001) but is not significantly associated with the basal with small correlation coefficient as 0.28 and p value as 0.08 (Table s1 and S2). For PYP +, global longitudinal strain is significantly strongly correlated with apical and mid regions but not with the basal region with strong Pearson correlation coefficient >0.8 and p value <.001 for apex and mid, while correlation coefficient as 0.22 (p=0.32) for basal. Apical region is significantly associated with mid with medium Pearson correlation coefficient as 0.55 (p=0.009) but not basal with p value as 0.44. Mid is not significantly associated with basal with p-value of 0.92. basal is not statistically associated with global, apex, and mid with p value all >0.05 (Tables S3 and S4).

Results

Patient demographics and variables

A total of 77 consecutive patients were identified, and 64 were included in the final analysis. The mean age of participants was 75.1 ± 2.9 years, ranging from 41 to 103 years. PYP+ patients were significantly older than PYP- patients (81.0 ±8.4 vs. 72.0 ±13.8, P=0.002). Males participants represented 89.1% of all participants, and there were no female participants in the PYP+ group, however, the sex distributions between the two groups were not statistically significant. LV septal (18.3 ± 3.0 vs. 14.1± 3.4 mm, P=0.0001) and posterior wall thickness (16.4 ± 2.6 vs. 13.1 ±3.0 mm, P=0.0004), LV mass (352.3 ±108.5 vs. 272.4 ±101.5 g, P=0.005) and LV mass index (175.7 ±51.8 vs. 137.2 ±42.5 g/m^2, P=0.002) were significantly higher in the PYP+ group. There was no difference in mortality rate between the two groups. Patient demographics and selected variables with a breakdown per PYP groups are outlined in **Table 1**.

Global and Regional Longitudinal Strain Comparison

The global, apical, mid, and basal regions were compared between participants with any ^{99m}Tc-PYP positivity and those with a completely negative scan (**Table 2**). The average global longitudinal strain (PYP+ vs. PYP-: -10.5 ± 2.6 vs. -13.1 ± 4.1, P= 0.003) and the average basal segment longitudinal strain (-4.6 ± 2.6 vs. -8.8±4.0, P<0.001) were significantly different between the PYP+ and PYP- groups; in which the PYP+ group had worse myocardial function. A trend was observed in the average mid-segment longitudinal strain (-9.6 ± 4.0 vs. -11.7± 4.4, P=0.07). In contrast, there was no statistical difference of the average apical longitudinal strain between the two groups (-17.6 ± 4.7 vs. -19.0 ± 6.5, P = 0.35). Relative apical longitudinal strain index (RALSI)

was found to be 1.3 ± 0.5 in PYP+ and 1.0 ± 0.3 in PYP- (P =0.008). The global and regional longitudinal strain analysis, along with RALSI, demonstrated overall worse myocardial function in PYP+ patients, with an apical sparing pattern.

Segment to segment comparison

Segment to segment analysis (**Table 3**) demonstrated a statistically significant difference in strain between PYP+ and PYP- segments in 4 segments: basal inferior (p=0.006), basal anterolateral (p= 0.01), apical septal (p=0.002) and apical inferior (p=0.001). No other segments demonstrated statistically significant difference. Of note, the segments with significant difference in strain were located either in the basal or the apical segments.

Comparison of Left Ventricular Diastolic Dysfunction

Left ventricular diastolic dysfunction was significantly different with 17 (77.3%) patients in group PYP+ versus 15 (36.6%) in PYP- participants (p = 0.002). When comparing the PYP+ group to the PYP- group, the medial E/e' ratio was significantly higher, and the mean mitral A wave velocity, medial and lateral e' velocity measurements were significantly lower. Also, we observed trends of higher mean E/A ratio and lateral E/e' ratio in the PYP+ group. These data consistently demonstrated worse diastolic function in PYP+ patients. Detailed data are summarized in **Table 4**.

Discussion

Our patient cohort has a similar age, sex and race distribution of CA patients compared to published data (*10, 21-23*); the absence of female cases in the PYP+ group is likely due to the small sample size, as PYP+ is known to have a male predominant population according to previous reports. LV mass and LV mass index were significantly higher in PYP+ patients. Of note, PYP+ patients were older than PYP- patients. To the best of our knowledge, this is the first study that demonstrated the difference of global and regional strain pattern among TTR subtype cardiac amyloidosis determined by ^{99m}Tc-PYP study and provided segment-to-segment comparison between PYP+ and PYP- segments. Our observation showed the correlations between ^{99m}Tc-PYP uptake and myocardial strain function impairment and provided insight of the underlying mechanism.

Correlations between ^{99m}Tc-PYP uptake and myocardial strain function impairment

Our result demonstrated overall compromised myocardial strain function and the basal-to-apex gradient (apical sparing) in both PYP+ and PYP- groups, which is consistent with prior studies and again supports the concept of apical sparing regardless of the background pathogenesis of CA (*10,11,24-25*). On top of that, our study further provided head-to-head comparison between the two groups and revealed significantly worse LVGLS and the basal regional strain in the PYP+ group, with a trend of worse mid ventricular regional strain and relatively spared apical regional strain. This is also reflected by the significantly higher RALSI in the PYP+ group, which indicates

a larger gradient of longitudinal strain. In the segment-to-segment comparison, the PYP+ segments generally had worse segmental strain function, despite not reaching statistical significance in every segment.

Our findings provided qualitative evidence for the correlations between ^{99m}Tc-PYP uptake and impaired myocardial strain function in patients with suspected CA. A recent European study found that quantified ^{99m}Tc-HMDP uptake in patients with TTR-related CA has a similar apical-sparing pattern as strain echo imaging (*13*), and suggested higher amyloid burden in the basal region being the underlying mechanism. Our study supports the concept, and further provided a head-to-head comparison of the nuclear tracer uptake and strain function, as echocardiography was not performed in their study.

We also attempted to compare our results with prior studies that assessed myocardial strain function in different subtypes of CA. However, due to lack of endomyocardial biopsy results to confirm the certain subtype, it is difficult to directly compare our results to these studies. Our PYP+ group contains TTR-related CA, however, this population can still include wild-type TTR (wt-TTR) and hereditary TTR (m-TTR), that may present with different LV strain function (*10*). Quarta et al reported better LVGLS in patients with m-TTR (-15% ± 4%) compared to wt-TTR (-11% ± 3%) and AL-type TTR (-12% ± 4%) in 172 endomyocardial biopsy confirmed patients (*10*). Our PYP+ group has a mean LVGLS that is similar to the wt-TTR group. Compared to Quarta's report, our PYP+ patients were 5-6 years older, and had higher LV mass index and mildly impaired LV ejection fraction (*10*), which can represent more severe phenotypes of the disease, and therefore related to worse LVGLS. Another study reported that there was no difference of LVGLS between three major subtypes (AL, wt-TTR and m-TTR) of CA, with impaired LVGLS strain at about -10% (*11*). Surprisingly, despite having worse LVGLS across all three groups, the LV ejection fraction were all within normal range in their study. The above studies reflected that patients with m-TTR could have a heterogeneous presentation concerning their LVGLS, this may provide an explanation for our observation of worse LVGLS in the PYP+ group.

Longitudinal strain impairment is known to be correlated to amyloid burden measured by histopathology staining, and late-gadolinium enhancement on cardiac magnetic resonance images (*11*). Our observation suggested that longitudinal strain impairment is also related to ^{99m}Tc-PYP uptake from segmental to global level. Although the exact mechanism of PYP uptake remains unclear, a potential mechanism such as microcalcification of the myocardial tissue may play a role in the development of strain function impairment (*14*). This is also supported by Gucht et al, who observed an apical-sparing pattern of Tc99m-HMDP uptake (*13*).

The investigational amyloid PET agents in clinical trials and literature have provided encouraging value in the diagnosis and investigation of cardiac amyloidosis. However, there is still a lack of convincing clinical evidence in distinguishing TTR CA from AL CA (25).

In brief, despite having similar compromised GLS and basal-to-apex regional strain gradient pattern, the overall worse global strain function and higher RALSI can potentially be used to characterize PYP+ patients. With the advantage of readily available and radiation free, speckle-tracking strain imaging can become a more valuable non-invasive diagnostic tool in the assessment of CA by providing additional subtyping and prognostic information prior to advanced imaging study such as ^{99m}Tc-PYP.

Diastolic Dysfunction in PYP+ patients

While the apical-sparing strain pattern is characteristic in CA patients, diastolic dysfunction also plays an important role in their clinical presentation and can independently predict mortality (*26*). Diastolic dysfunction in CA patients has been observed in early studies and can deteriorate with progression of the disease (*27,28*). In the PYP+ group, we observed significantly worse diastolic function measured by E/A ratio, medial and lateral e' velocity, and E/e' ratio compared to the PYP- group. To the best of our knowledge, this is the first report that compares PYP+ and PYP- patients, and our findings indicate that ^{99m}Tc-PYP uptake can be a surrogate marker for worse cardiac diastolic function patients with suspected CA. Again, the significantly older age in our PYP+ group may reflect a later stage of the disease, so this result should be interpreted carefully.

Limitations

The study is limited by its retrospective, single center design. The relatively low number of participants is due to the strict enrollment criteria of participants undergoing PYP scan and strain imaging within 90 days from a single center. To sufficiently power future similar studies participants will likely need to be enrolled from multiple centers. The comparison of strain imaging utilizing the 18-segment model and PYP imaging using the 17-segment model was troublesome; and may significantly compromise the segment-to-segment comparison of the apical strain. Efforts were made in the study to negate this discrepancy as much as possible. The intervals between PYP injection and scintigraphy scan can lead to different false positive rates among different protocols, so generalization of our results to different scanning protocols needs to be cautious.

With limited endomyocardial biopsy results, we were not able to further identify the patients in the PYP+ group as hereditary- or wild-type TTR, which may present with different levels of myocardial strain dysfunction.

Conclusion

With the advance of imaging technology, noninvasive approaches such as ^{99m}Tc-PYP imaging has become an essential part in the diagnosis of cardiac amyloidosis, without the need of endomyocardial biopsy. Our study suggested that PYP uptake is related to overall worse LV segmental, regional and global longitudinal strain function, as well as diastolic function compared to patients without PYP uptake. Our work provides important data for clinicians to appreciate the echocardiographic features related to ^{99m}Tc-PYP uptake and can serve as a hypothesis-generating study for future investigators.

KEY POINTS:

Question: How does ^{99m}Tc-pyrophosphate (PYP) and echocardiographic strain imaging compare on the assessment of transthyretin (TTR) cardiac amyloidosis?

Pertinent Findings: Our study suggested that PYP uptake is related to overall worse LV segmental, regional, and global longitudinal strain function, as well as diastolic function compared to patients without PYP uptake.

Implications for Patient Care: This provides important data for clinicians to know the echocardiographic function features related to ^{99m}Tc-PYP uptake and can serve as a hypothesis-generating study for future investigators.

References:

1. Dubrey SW, Hawkins PN, Falk RH. Amyloid diseases of the heart: assessment, diagnosis, and referral. *Hear Br Cardiac Soc* 2011;97:75–84.

2. Larsen BT, Mereuta OM, Dasari S, et al Correlation of histomorphological pattern of cardiac amyloid deposition with amyloid type: a histological and proteomic analysis of 108 cases. *Histopathology* 2015;68:648–656.

3. Maleszewski JJ. Cardiac amyloidosis: pathology, nomenclature, and typing. *Cardiovasc Pathology Official J Soc Cardiovasc Pathology* 2015;24:343–350.

4. Gertz MA, Comenzo R, Falk RH, et al Definition of organ involvement and treatment response in immunoglobulin light chain amyloidosis (AL): a consensus opinion from the 10th international symposium on amyloid and amyloidosis. *Am J Hematol* 2005;79:319–328.

5. Ruberg FL, Grogan M, Hanna M, Kelly JW, Maurer MS. Transthyretin amyloid cardiomyopathy. *J Am Coll Cardiol* 2019;73:2872–2891.

6. Williams LK, Frenneaux MP, Steeds RP. Echocardiography in hypertrophic cardiomyopathy diagnosis, prognosis, and role in management. *Eur J Echocardiogr* 2009;10:iii9–iii14.

7. Pagourelias ED, Mirea O, Duchenne J, et al. Echo parameters for differential diagnosis in cardiac amyloidosis. *Circulation Cardiovasc Imaging* 2017;10:e005588.

8. Phelan D, Collier P, Thavendiranathan P, et al Relative apical sparing of longitudinal strain using two-dimensional speckle-tracking echocardiography is both sensitive and specific for the diagnosis of cardiac amyloidosis. *Hear Br Cardiac Soc* 2012;98:1442–1448.

9. Liu D, Hu K, Nordbeck P, Ertl G, Störk S, Weidemann F. Longitudinal strain bull's eye plot patterns in patients with cardiomyopathy and concentric left ventricular hypertrophy. *Eur J Med Res* 2016;21:21.

10. Quarta CC, Solomon SD, Uraizee I, et al. Left ventricular structure and function in transthyretin-related versus light-chain cardiac amyloidosis. *Circulation* 2014;129:1840–1849.

11. Ternacle J, Bodez D, Guellich A, et al. Causes and consequences of longitudinal LV dysfunction assessed by 2D strain echocardiography in cardiac amyloidosis. *Jacc Cardiovasc Imaging* 2016;9:126–138.

12. Perugini E, Guidalotti PL, Salvi F, et al. Noninvasive Etiologic Diagnosis of Cardiac Amyloidosis Using 99m Tc-3,3-Diphosphono-1,2-Propanodicarboxylic Acid Scintigraphy. *J Am Coll Cardiol* 2005;46:1076–1084.

13. Gucht AVD, Cottereau A-S, Abulizi M, et al. Apical sparing pattern of left ventricular myocardial (99m)Tc-HMDP uptake in patients with transthyretin cardiac amyloidosis. *J Nucl Cardiol Official Publ Am Soc Nucl Cardiol* 2017;25:2072–2079.

14. Stats MA, Stone JR. Varying levels of small microcalcifications and macrophages in ATTR and AL cardiac amyloidosis: implications for utilizing nuclear medicine studies to subtype amyloidosis. *Cardiovasc Pathol* 2016;25:413–417.

15. Ronald M. Witteles, Michaela Liedtke. AL Amyloidosis for the Cardiologist and Oncologist: Epidemiology, Diagnosis, and Management, JACC: CardioOncology, 2019 (1)1 117-13 https://doi.org/10.1016/j.jaccao.2019.08.002.

16. Nagueh SF, Smiseth OA, Appleton CP, et al. Recommendations for the Evaluation of Left Ventricular Diastolic Function by Echocardiography: An Update from the American Society of Echocardiography and the European Association of Cardiovascular Imaging. J Am Soc Echocardiogr. 2016 Apr;29(4):277-314. doi: 10.1016/j.echo.2016.01.011.

17. Lang RM, Badano LP, Mor-Avi V, et al. Recommendations for Cardiac Chamber Quantification by Echocardiography in Adults: An Update from the American Society of Echocardiography and the European Association of Cardiovascular Imaging. *J Am Soc Echocardiog* 2015;28:1-39.e14.

18. Cerqueira MD, Weissman NJ, Dilsizian V, et al. American Heart Association Writing Group on Myocardial Segmentation and Registration for Cardiac Imaging. Standardized myocardial segmentation and nomenclature for tomographic imaging of the heart. A statement for healthcare professionals from the Cardiac Imaging Committee of the Council on Clinical Cardiology of the American Heart Association. Circulation. 2002 Jan 29;105(4):539-42. doi: 10.1161/hc0402.102975.

19. Bokhari S, Castaño A, Pozniakoff T, Deslisle S, Latif F, Maurer MS. (99m)Tc-pyrophosphate scintigraphy for differentiating light-chain cardiac amyloidosis from the transthyretin-related familial and senile cardiac amyloidoses. Circ Cardiovasc Imaging. 2013 Mar 1;6(2):195-201. doi: 10.1161/CIRCIMAGING.112.000132. Epub 2013 Feb 11. PMID: 23400849; PMCID: PMC3727049.

20. Dorbala S, Ando Y, Bokhari S, Dispenzieri A, et al. ASNC/AHA/ASE/EANM/HFSA/ISA/SCMR/SNMMI expert consensus recommendations for multimodality imaging in cardiac amyloidosis: Part 1 of 2—evidence base and standardized methods of imaging. *J Nucl Cardiol* 2019;26:2065–2123.

21. Sperry BW, Vranian MN, Hachamovitch R, Joshi H, Ikram A, Phelan D, Hanna M. Subtype-specific interactions and prognosis in cardiac amyloidosis. *J Am Heart Assoc* 2016;5:e002877.

22. Pinney JH, Whelan CJ, Petrie A, et al. Senile systemic amyloidosis: clinical features at presentation and outcome. *J Am Heart Assoc* 2013;2:e000098.

23. Connors LH, Sam F, Skinner M, et al. Heart Failure Resulting From Age-Related Cardiac Amyloid Disease Associated With Wild-Type Transthyretin. *Circulation* 2016;133:282–290.

24. Nardozza M, Chiodi E, Mele D. Left Ventricle Relative Apical Sparing in Cardiac Amyloidosis. *J Cardiovasc Echography* 2017;27:141–142.

25. Yang M, Arsanjani R, Roarke MC. Advanced Nuclear Medicine and Molecular Imaging in the Diagnosis of Cardiomyopathy. AJR Am J Roentgenol. 2020 Nov;215(5):1208-1217. doi: 10.2214/AJR.20.22790. Epub 2020 Sep 9. PMID: 32901569.

26. Chacko L, Martone R, Bandera F, et al Echocardiographic phenotype and prognosis in transthyretin cardiac amyloidosis. *Eur Heart J* 2020;41:1439–1447.

27. Hartmann A, Frenkel J, Hopf R, et al. Is technetium-99 m-pyrophosphate scintigraphy valuable in the diagnosis of cardiac amyloidosis? *Int J Cardiac Imaging* 1990;5:227–231.

28. Klein AL, Hatle LK, Burstow DJ, Seward JB, Kyle RA, Bailey KR, Luscher TF, Gertz MA, Tajik AJ. Doppler characterization of left ventricular diastolic function in cardiac amyloidosis. *J Am Coll Cardiol* 1989; 13:1017–1026.

Figure 1. Side-by-side comparison of ^{99m}Tc-PYP scan and speckle-tracking strain imaging in a representative case with positive PYP scan.

AHA 17-segment model bull's eye color-mapping plots of ^{99m}Tc-PYP scan (Figure 1A) and speckle-tracking strain imaging (Figure 1B). Figure 1A demonstrates intense left ventricular myocardium ^{99m}Tc-PYP uptake in the anterior and inferior segments, and no ^{99m}Tc-PYP uptake at the apex. Figure 1B demonstrates the characteristic apical-sparing distribution pattern of peak left ventricular longitudinal systolic strain. In this case, the segments with ^{99m}Tc-PYP uptake is associated with worse strain function. The values in the Figure 1A stand for segmental peak longitudinal systolic strain of each segment. Ant: anterior, Lat: lateral, Post: posterior, Inf: inferior, Sept: septal.

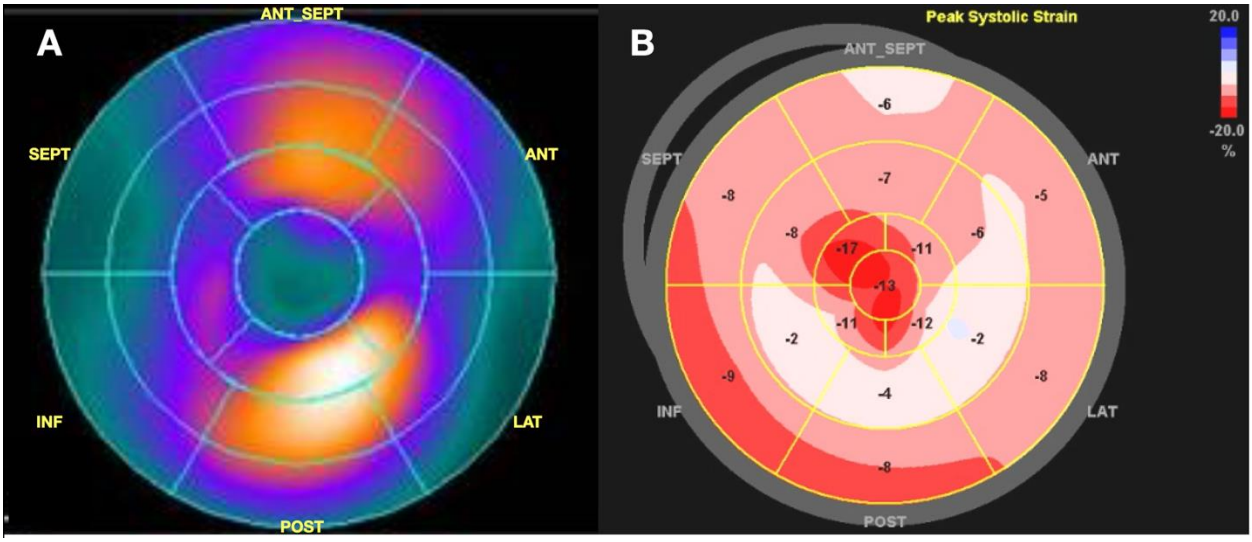

Table 1. Patient Demographics

	PYP+(n=22)	PYP-(n=42)	Total (n=64)	P Value
Age (mean, SD)	81.0 (8.4)	72.0 (13.8)	75.1 (12.9)	0.002*
Gender, Male (n, %)	22 (100.0%)	35 (83.3%)	57 (89.1%)	0.09**
BMI (mean, SD)	27.0 (3.5)	27.2 (5.3)	27.1 (4.8)	0.89*
Systolic blood pressure (mmHg) (mean, SD)	119.8 (16.4)	136.6 (27.5)	130.6 (25.3)	0.029**
Diastolic blood pressure (mmHg) (mean, SD)	73.7 (11.93)	80.5 (15.73)	78.1 (14.74)	0.070**
Hypertension (n, %)	12 (63.2%)	25 (73.5%)	37 (69.8%)	0.536**
History of CAD (n, %)	6 (31.6%)	10 (29.4%)	16 (30.2%)	1.000**
History of DM (n, %)	2 (10.5%)	10 (29.4%)	12 (22.6%)	0.174**
Beta-blocker (n, %)	10 (52.6%)	22 (64.7%)	32 (60.4%)	0.559**
CCB (n, %)	1 (5.3%)	9 (26.5%)	10 (18.9%)	0.076**
ACE-I (n, %)	3 (15.8%)	5 (14.7%)	8 (15.1%)	1.000**
ARB (n, %)	5 (26.3%)	5 (14.7%)	10 (18.9%)	0.465**
Spironolactone (n, %)	4 (21.1%)	5 (14.7%)	9 (17.0%)	0.706**
Amiodarone (n, %)	0 (0.0%)	1 (2.9%)	1 (1.9%)	1.000**
Creatine (median, IQR)	1.3 (1.1, 1.5)	1.3 (1.1, 1.8)	1.3 (1.1, 1.7)	0.44***
NT-proBNP (median, IQR)	3095.0(1640.0, 7323.0)	3097.0(1238.5, 8832.5)	3097.0(1407.0, 7447.0)	0.99***
Low Voltage on ECG (n, %)	6 (28.6%)	5 (11.9%)	11 (17.5%)	0.1575**
LV septal wall thickness (mm), (mean, SD)	18.3 (2.96)	14.1 (3.43)	15.7 (3.83)	0.0001*
LV posterior wall thickness (mm), (mean, SD)	16.4 (2.63)	13.1 (2.99)	14.3 (3.28)	0.0004*
LV Mass (g) (mean, SD)	352.3 (108.5)	272.4 (101.5)	300.7 (110.1)	0.005*
LV Mass Index (g/m2)(mean, SD)	175.7 (51.8)	137.2 (42.5)	150.4 (49.1)	0.002*
LV End-Diastolic diameter (mm), (mean, SD)	44.5 (6.69)	47.2 (6.95)	46.2 (6.91)	0.143*
Ejection Fraction % (mean, SD)	47.9 (15.2)	51.8 (15.2)	50.5 (15.2)	0.34*
Stroke volume (ml) (mean, SD)	65.6 (25.7)	76.4 (25.1)	72.5 (25.6)	0.1146***
Cardiac index (L/m2/min)	2.4 (0.83)	2.8 (0.88)	2.6 (0.88)	0.075**
TAPSE by M-mode (mm), (mean, SD)	12.3 (3.30)	17.2 (5.36)	15.8 (5.29)	0.0250***
Pericardial effusion (n, %)	8 (36.4%)	6 (14.3%)	14 (21.9%)	0.0584**
H/CL ratio	1.7 (0.4)	1.1 (0.2)	1.3 (0.4)	<0.001*
PYP Scale †	0 (0.0%)	30 (71.4%)	30 (46.9%)	<0.001**
0	2 (9.1%)	7 (16.7%)	9 (14.1%)	
1	6 (27.3%)	2 (4.8%)	8 (12.5%)	
2	14 (63.6%)	3 (7.1%)	17 (26.6%)	
3	0 (0.0%)	30 (71.4%)	30 (46.9%)	

* Unequal variance two-sample t-test, ** Fisher's exact test, ***Wilcoxon rank sum test.

† The qualitative value for interpretation is determined by comparing the uptake in the myocardium, grade 0 = no myocardial uptake, grade 1= myocardial uptake less than bone uptake, grade2= myocardial uptake equal to bone uptake, grade 3= myocardial uptake greater than bone uptake.

Table 2. Regional comparison in PYP+ versus PYP- participants utilizing the 17-segment model.

Region	PYP + (n=22)	PYP - (n=42)	Total (n=64)	P Value*
Global (%)	-10.5 (2.6)	-13.1 (4.1)	-12.2 (3.9)	0.003
Apex (%)	-17.6 (4.7)	-19.0 (6.5)	-18.5 (5.9)	0.35
Mid (%)	-9.6 (4.0)	-11.7 (4.4)	-11.0 (4.6)	0.07
Basal (%)	-4.6(2.6)	-8.8 (4.0)	-7.3 (4.1)	<0.001

*Two-sample t-test

Table 3. Segment to segment comparison in PYP+ versus PYP- participants utilizing the 17-segment model individually.

Segment		PYP-		PYP+		P Value*
		N	Mean (SD), %	N	Mean (SD), %	
Basal	Anterior	49	-8.5 (6.82)	12	-5.7 (4.31)	0.17
	Anteroseptal	54	-13.3 (7.58)	8	-14.3 (6.86)	0.73
	Inferoseptal	50	-19.3 (8.09)	9	-20.3 (7.55)	0.71
	Inferior	44	-8.7 (6.44)	16	-3.3 (6.27)	0.006
	Inferolateral	46	-11.7 (8.40)	15	-10.9 (6.51)	0.74
	Anterolateral	51	-19.7 (8.63)	9	-11.8 (8.57)	0.01
Mid	Anterior	45	-8.3 (6.00)	18	-6.3 (4.69)	0.20
	Anteroseptal	40	-10 (5.92)	21	-8.4 (4.63)	0.31
	Inferoseptal	41	-18.9 (8.91)	22	-18.0 (5.69)	0.61
	Inferior	45	-9.4 (8.64)	18	-7.6 (6.12)	0.42
	Inferolateral	48	-9.1 (6.12)	14	-7.9 (4.07)	0.52
	Anterolateral	49	-16.4 (8.25)	14	-15.6 (6.44)	0.76
Apical	Anterior	51	-12.4 (4.80)	12	-10.2 (3.09)	0.15
	Septal	41	-13.1 (4.96)	22	-9.9 (2.85)	0.002
	Inferior	42	-13.1 (4.90)	21	-9.7 (2.80)	0.001
	Lateral	51	-12.4 (4.76)	12	-10.2 (3.31)	0.13
	Apex	55	-12.2 (4.67)	8	-10.5 (3.83)	0.33

*Two-sample t-test

Table 4. Left ventricular diastolic function parameters.

	PYP+ (N=22)	PYP - (N=42)	Total (N=64)	P Value
Presence of diastolic dysfunction (n, %)	17 (77.3%)	15 (36.6%)	32 (50.0%)	0.002*
Peak Tricuspid Regurgitation velocity (m/s), (mean, SD)	2.7 (0.44)	2.9 (0.46)	2.8 (0.46)	0.176**
Right ventricular systolic pressure (mmHg), (mean, SD)	40.3 (12.7)	44.1 (15.1)	42.8 (14.3)	0.3370***
E-wave velocity (m/s) (median, IQR)	0.9 (0.8, 1.0)	0.8 (0.7, 1.0)	0.9 (0.7, 1.0)	0.70**
A-wave velocity (m/s) (median, IQR)	0.5 (0.3, 0.7)	0.8 (0.6, 0.9)	0.7 (0.5, 0.9)	0.03**
E/A ratio (median, IQR)	2.0 (1.1, 3.0)	1.2 (0.9, 1.8)	1.3 (1.0, 2.0)	0.06**
E deceleration time (ms) (median, IQR)	154.5 (140.0, 189.0)	178.0 (139.0, 205.0)	170.0 (140.0, 205.0)	0.46**
Tissue doppler Medial e'> velocity (cm/s) (mean, SD)	3.3 (1.9)	4.7 (1.7)	4.2 (1.9)	0.009**
Tissue doppler Lateral e'> velocity (cm/s) (mean, SD)	4.4 (2.0)	6.3 (2.3)	5.6 (2.4)	0.009**
E/e' ratio Medial (mean, SD)	32.4 (18.3)	22.0 (12.1)	25.8 (15.3)	0.02***
E/e' ratio Lateral (mean, SD)	21.8 (9.2)	17.0 (10.3)	18.8 (10.1)	0.07***

* Fisher's exact test, ** Wilcoxon rank sum p-value, *** Two sample t-test

Supplementary Material

For PYP- participants, global longitudinal strain is significantly strongly correlated with apical, mid, and basal regions with Pearson correlation coefficient >0.6 and p value <.001. The apical region is significantly strongly associated with mid region, with correlation of 0.7 (p<.001) but is not significantly associated with the basal with small correlation coefficient as 0.28 and p value as 0.08 (Table s1 and S2). For PYP +, global longitudinal strain is significantly strongly correlated with apical and mid regions but not with the basal region with strong Pearson correlation coefficient >0.8 and p value <.001 for apex and mid, while correlation coefficient as 0.22 (p=0.32) for basal. Apical region is significantly associated with mid with medium Pearson correlation coefficient as 0.55 (p=0.009) but not basal with p value as 0.44. Mid is not significantly associated with basal with p-value of 0.92. basal is not statistically associated with global, apex, and mid with p value all >0.05 (Tables S3 and S4).

Table S1 Pearson correlation coefficient for PYP- groups (Global, apex, mid, basal).

Pearson Correlation Coefficients, N = 41 Prob > |r| under H0: Rho=0				
	Global	**Apex**	**Mid**	**Basal**
Global	1.00000	0.87 <.0001	0.89 <.0001	0.64 <.0001
Apex	0.87 <.0001	1.00	0.71 <.0001	0.28 0.08
Mid	0.89 <.0001	0.71 <.0001	1.00	0.46 0.003
Basal	0.64 <.0001	0.28 0.08	0.46 0.003	1.00

Table S2 - Matrix scatter plot (PYP-).

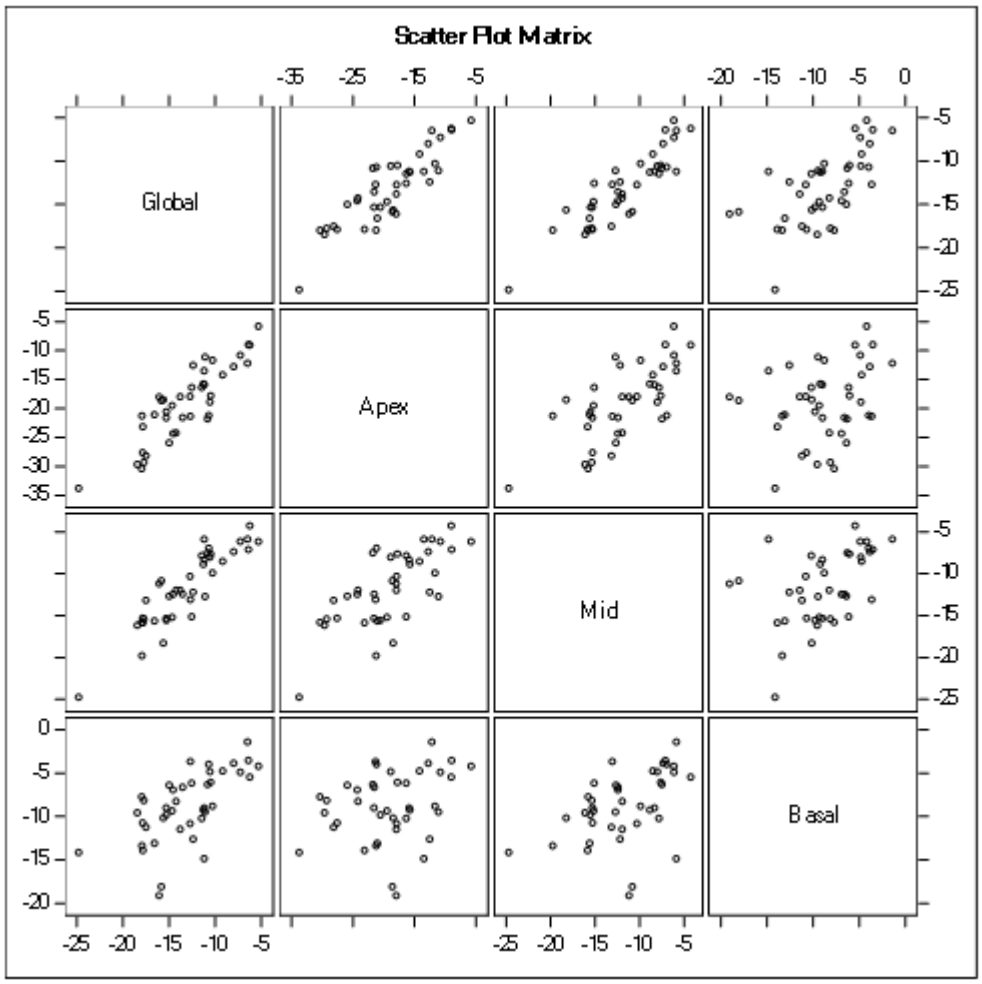

Table S3 Pearson correlation coefficient for PYP+ groups (Global, apex, mid, basal).

Pearson Correlation Coefficients, N = 22 Prob > |r| under H0: Rho=0				
	Global	**Apex**	**Mid**	**Basal**
Global	1.00	0.81 <.0001	0.84 <.0001	0.22 0.32
Apex	0.81 <.0001	1.00	0.55 0.009	-0.17 0.44
Mid	0.84 <.0001	0.55 0.009	1.00	-0.02 0.92
Basal	0.22 0.32	-0.17 0.44	-0.02 0.92	1.00

Table 4 matrix scatter plot (PYP+).